Electronic Supplementary Material (ESI) for Chemical Communications.

Electronic Supplementary Information

A platform for development of novel biosensors by configuring allosteric transcription factor recognition with amplified luminescent proximity homogeneous assay

Shanshan Li,[a] Li Zhou,[b] Yongpeng Yao,[a] Zilong Li,[a] Keqiang Fan,[a] Lixin Zhang,[ab] Weishan Wang,*[a] and Keqian Yang*[a]

[a] State Key Laboratory of Microbial Resources, Institute of Microbiology, Chinese Academy of Sciences, 100101 Beijing, China.

[b] Institute of Health Sciences, Anhui University, 230601, Hefei, China.

* Corresponding authors:

Keqian Yang: yangkq@im.ac.cn

Weishan Wang: wangws@im.ac.cn

Contents

Materials and Methods

Regents. The donor and acceptor beads were purchased from PerkinElmer (No. 6760619). Uric acid (UA), oxytetracycline (OTC), chlortetracycline (CTC), tetracycline (TC), anhydrotetracycline (ATC), amino acids, bovine albumin (BSA) used in this work were purchased from Sigma. Human serum samples were purchased from Beijing Solarbio Science & Technology Co., Ltd. and Beijing LabLead Biotech Co., Ltd.. The other chemicals were of analytical grade and purchased from Aladdin. Unless specified, for all buffers, 0.005 % Tween-20 and 0.1% BSA were added, pH was adjusted to 7.4. Other ingredients in different buffers were described as follows. HBS-P buffer contained 10 mM 4-(2-hydroxyethyl)-1-piperazineethanesulfonic acid (HEPES), 15 mM sodium chloride; HBS-EP buffer contained extra 3 mM ethylenediaminetetraacetic acid (EDTA) than HBS-P buffer; PBS-P buffer (0.1 M, 100 mL) was prepared by mixing 81 mL disodium hydrogen phosphate (0.1 M) and 19 mL sodium dihydrogen phosphate (0.1 M); AH buffer contained 25 mM HEPES, 20 mM sodium chloride. UA was dissolved in 0.5 M sodium hydroxide to a concentration of 0.1 M. Guanine was dissolved in 0.1 M sodium hydroxide to a concentration of 0.1 mM. Hypoxanthine and xanthine were dissolved in 0.1 M potassium hydroxide to a concentration of 0.1 mM. Adenine was dissolved in deionized water to a concentration of 0.1 mM.

DNA manipulation. General DNA manipulations were performed as described.[1] PCRs were performed with Taq DNA polymerase (TransGene, Beijing, China) according to the manufacturer's instructions. All PCR primers used in this study are listed in Table S1.

Cloning, expression, and purification of HucR and OtrR. *Escherichia coli* TOP 10 was used as a host strain for cloning experiments. To express HucR, *hucR* gene was amplified from the genomic DNA of *Deinococcus radiodurans* with a primer pair RF/RR. The PCR product was digested with NdeI/XhoI and inserted into the corresponding restriction enzyme sites of plasmid pET-23b (Novagen) to generate plasmid pET-HucR. Then the resulting plasmid was transformed into *E. coli* BL21 (DE3) to express HucR. The expression and purification of HucR were performed as previously described.[2] Purity of HucR was verified by sodium dodecyl sulfate-polyacrylamide gel electrophoresis (SDS-PAGE) (Fig. S1). The expression and purification of OtrR were performed as previously described.[3] Purified

OtrR was verified by SDS-PAGE (Fig. S10a).

Preparation of biotinylated DNA containing *hucO* (Bio-*hucO*) and their mutants. Bio-*hucO* and their mutants were amplified by two rounds of PCR. First, unlabeled DNA sequence containing *hucO* and their mutants were amplified by overlap PCR using the same forward primer OF and different reverse primers from OR0 to OR23 (Table S1). Then, the biotinylated products were prepared by a second round of PCR, using the PCR products generated from the first round as templates, and the corresponding primer pairs from BioP/OR0 to BioP/OR23. The final PCR products of Bio-*hucO* and their mutants were purified by gel extraction kit (Axygen), verified by agarose gel electrophoresis, and quantified by NanoVue plus (GE Healthcare).

Preparation of biotinylated DNA sequence containing *otrO* (Bio-*otrO*) and its mutants. Bio-*otrO* and its mutants Bio-*otrO*-1, Bio-*otrO*-2, and Bio-*otrO*-3 were prepared by overlap PCR using the same forward primer BioP and different reverse primer otrOR, otrO1 otrO2, and otrO3 (Table S1), respectively. Then the PCR products were purified by gel extraction kit (Axygen), verified by agarose gel electrophoresis, and quantified by NanoVue plus (GE Healthcare).

Electrophoresis mobility shift assay (EMSA). Binding between HucR and *hucO* was primarily assayed by EMSA (Fig. S2). The *hucO* probe (P-hucO) used for EMSA was obtained by PCR with primer pair P-hucOF/P-hucOR and genomic DNA of *D. radiodurans*. Experiment conditions for EMSA and data recording were same as described previously.[2]

Bio-layer interferometry (BLI) assay. Kinetics between aTF (HucR and OtrR) and its target binding site (TFBS; *hucO* and *otrO*) was determined by BLI technology using an Octet RED96 system (FortéBIO) (Fig. S3, S7, S10b and S12). Briefly, the whole process contained five steps: balance, DNA loading, rebalance, association, and dissociation.[4] HBS-EP buffer was used for baseline balance and sample dilution. The blank tests were carried out by using HBS-EP buffer instead of aTFs in the association step and used for baseline correction. Kinetic parameters (Table S3 and S6), association rate constant k_{on}, dissociation rate constant k_{off}, and equilibrium dissociation constant K_D ($K_D = k_{off}/k_{on}$)

were calculated by fitting the processed data (baseline correction and normalization) with a 1:1 model using Octet Analysis System 21 CFR Part 11 (version 9.0).

Luminescence output assay. Measurements of luminescence generated by the biosensors (the relative luminescence unit, RLU) were performed at room temperature in 384-well white OptiPlates (PerkinElmer; No. 6007299) as follows. First, the aTF (HucR or OtrR), biotinylated DNA sequence containing TFBS (Bio-*hucO*, Bio-*otrO* and their derivatives), and the target chemical (effector UA , OTC, and their respective structural analogues, if necessary) with the same volume (5 μL) were incubated together for 30 min; then, 5 μL of acceptor and donor beads were sequentially added to the final concentration of 20 μg/mL, and incubated in dark for 30 and 60 min, respectively; finally, luminescence signal was detected on EnSpire Multimode Plate Reader (PerkinElmer). Raw data were processed by subtracting the luminescence signal of the blank control. K_I (equilibrium dissociation constant between the analyte and aTF) and I_{50} (concentration of the analyte producing 50% signal reduction) were calculated with the in-built one-site fit K_I and one-site fit $LogI_{50}$ models of software GraphPad Prism (version 5.0), respectively. Limit of detection (LOD) of biosensor was the minimal concentration of UA where the declined luminescence signal (ΔRLU) is at least three times of the blank.[5]

Detection of UA in human urine and serum samples by high performance liquid chromatograph (HPLC). For HPLC assay, urine samples collected from healthy volunteers and commercial purchased serum samples were appropriately diluted with HBS-P buffer and filtrated through 0.22 μm cellulose acetate membrane. UA were analyzed by HPLC-20AT (Shimadzu) equipped with an SPD-20A UV detector. The analytical column was Zorbax SB-Aq (Agilent; 250 mm × 4.6 mm, 5 μm). The mobile phase consisting of 98% acetate (pH 3.2) and 2% methanol was run at a flow rate of 1.0 mL/min. The detection of UA was carried out by UV absorbance at 280 nm. Injection volume was 20 μL.

References

1 T. Kieser, M. J. Bibb, M. J. Buttner, K. F. Chater, D. A. Hopwood, *Practical Streptomyces Genetics*, The John

Innes Foundation, Norwich, UK, 2000.

2 J. Wang, W. Wang, L. Wang, G. Zhang, K. Fan, H. Tan, K. Yang, *Mol. Microbiol.*, 2011, **82**, 236-250.

3 W. Wang, T. Yang, Y. Li, S. Li, S. Yin, K. Styles, C. Corre, K. Yang, *ACS Syn. Biol.*, 2016, **5**, 765-773.

4 A. Levina, T. H. N. Pham, P. A. Lay, *Angew. Chem. Int. Ed.*, 2016, **55**, 8104-8107.

5 (a) Q. Long, A. Fang, Y. Wen, H. Li, Y. Zhang, S. Yao, *Biosens. Bioelectron.*, 2016, **86**, 10-114. (b) C. Zhang, S. Si, Z. Yang, *Biosens. Bioelectron.*, 2014, **65**, 115-120.

Mathematical modeling

LOD and linear range are two key parameters describing the performance of a biosensor. Hence, critical factors that affect the two parameters of the biosensor were first determined by mathematical modeling, which would provide guide to optimize the biosensor rationally. As shown in Fig. 3A, two major equilibriums existed in the biosensor,

$$aTF + DNA \overset{K_D}{\leftrightarrow} aTF\text{-}DNA$$

$$aTF + E \overset{K_I}{\leftrightarrow} aTF\text{-}E$$

where the first describes equilibrium between aTF and its TFBS, and the second shows equilibrium between aTF and the effector (the target chemical). Here, K_D and K_I are the affinities of aTF for DNA and effector, respectively.

Concentration of DNA is much higher (> 10-fold) than that of aTF in the biosensor.[1] Thus, binding of aTF to DNA (B_I) can be described by a competitive inhibit model as follows.

$$B_I = \frac{B_{max}[DNA]}{K_D\left(1 + \frac{[E]}{K_I}\right) + [DNA]} \qquad \text{Eq. (1)S}$$

where B_{max} is the maximal luminescence signal of the binding (Fig. S6a). Square bracket indicates the concentration of the corresponding substance. When the effector (E) is absent, binding of this system can be simplified to [Eq. (**2**)S].

$$B_0 = \frac{B_{max}[DNA]}{K_D + [DNA]} \qquad \text{Eq. (2)S}$$

Dissociation of aTF from its TFBS (B_{dis}) resulted from the binding between the effector and aTF can be described by [Eq. (**3**)S] derived from the Dose-response model.[2]

$$B_{dis} = B_{min} + \frac{B_{max}^{'} - B_{min}}{1 + 10^{\left(\log[E] - \log I_{50}\right)}} \qquad \text{Eq. (3)S}$$

where $B_{max}^{'}$ and B_{min} indicates the maximal and minimal luminescent signal of the dissociation curve, respectively (Fig. S6b). This dissociation curve suggests both sensitivity and linear range of the biosensor are related to I_{50} and the maximal slope k_{max} (Fig. 3A and S6b). Here, I_{50} equals to the concentration of the effector required for 50% signal reduction (Fig. S6b). Therefore, it is significant to make certain of factors influencing I_{50} and k_{max}.

When [E] = I_{50} and $B_0 = 2B_I$, [Eq. (**4**)S] deduced from [Eq. (**1**)S] and [Eq. (**2**)S] gave factors influencing I_{50} (Fig. 3A) as follows.

$$I_{50} = K_I\left(1 + \frac{[DNA]}{K_D}\right) \quad \text{Eq. (4)S}$$

Since the concentration of DNA was fixed in the biosensor, it could be clearly seen from [Eq. (**4**)S] that I_{50} is positively related to K_I, and negatively related to K_D.

The maximal slope k_{max} was obtained by taking the derivative of [Eq. (**3**)S] at the point of [E] = I_{50} (Fig. 3A) as follows.

$$k_{max} = -\ln(10) \times (B'_{max} - B_{min}) \quad \text{Eq. (5)S}$$

[Eq. (**5**)S] showed that linear range of this biosensor is related to the difference value between the maximal and minimal luminescence signal of the dissociation curve. Actually, B'_{max} is the luminescence signal when effector is absent, so it can be expressed by [Eq. (**2**)S]. Thus, [Eq. (5)S] could be also expressed as follows.

$$k_{max} = -\ln(10) \times \left(\frac{B_{max}[DNA]}{K_D + [DNA]} - B_{min}\right) \quad \text{Eq. (6)S}$$

As shown in [Eq. (**6**)S], k_{max} is theoretically positively related to K_D. So either reducing I_{50} or increasing k_{max} could lower LOD and broaden linear range of the biosensor (Fig. S6). As analyzed above, these objectives could be achieved by reducing the affinity (increasing K_D) between aTF and TFBS, or increasing the affinity between aTF and effector (reducing K_I). Since DNA binding affinity of a protein could be changed by engineering this protein or its TFBS,[3, 4] our goals could be attained by mutating aTFs (HucR and OtrR) or their TFBS (*hucO* and *otrO*). To obtain an ideal mutation of aTF with both increased K_D and reduced K_I requires complex protein engineering and laborious screening of mutants. In contrast, mutation of TFBS that just affects K_D is much easier, so it was preferred for biosensor optimization.

References

1 C. Yung-Chi, W. H. Prusoff, *Biochem. Pharmacol.*, 1973, **22**, 3099-3108.

2 K. S. Crump, D. G. Hoel, C. H. Langley, R. Peto, *Cancer Res.*, 1976, **36**, 2973-2979.

3 O. Hallikas, J. Taipale, *Nat. Protocols*, 2006, **1**, 215-222.

4 S. Akashi, R. Osawa, Y. Nishimura, *J. Am. Soc. Mass Spect.*, 2005, **16**, 116-125.

Supporting figures

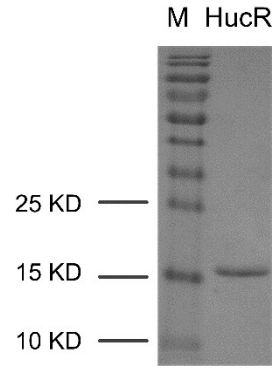

Fig. S1. Purified HucR examined by SDS-PAGE. Lane M, protein markers (10-180 KDa). HucR, purified His_6-tagged HucR.

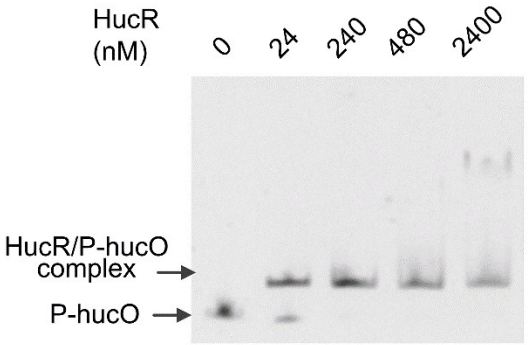

Fig. S2. EMSA of the binding of HucR with P-hucO. P-hucO (6 ng) was titrated by HucR with different concentrations (0, 24, 240, 480, and 2400 nM). The first lane without HucR was the control.

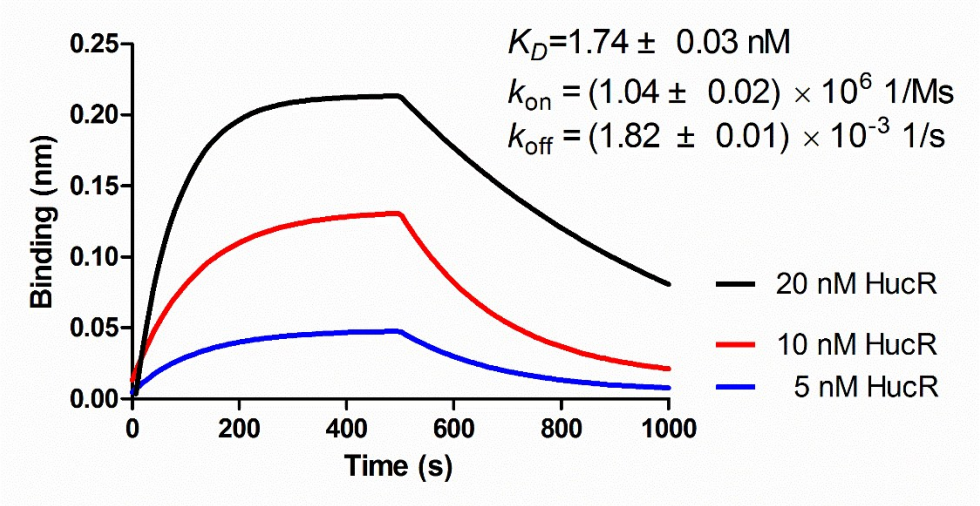

Fig. S3. Determination of the kinetics of HucR for *hucO* by BLI. The Bio-*hucO* (10 ng/μL) was loaded on the streptavidin sensor, and then interacted with HucR at three different concentrations of 5 nM (blue line), 10 nM (red line), and 20 nM (black line). The blank experiment for data correction was carried out by using HBS-EP buffer instead of HucR in the binding step.

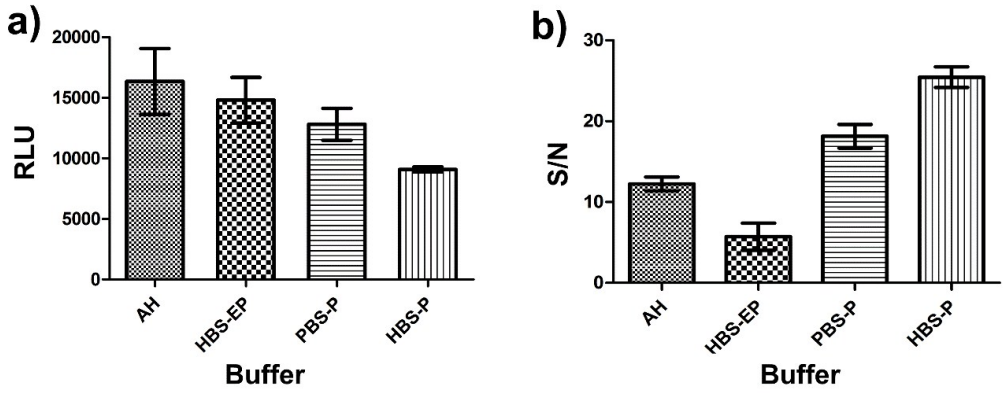

Fig. S4. Evaluation of influence of different buffers on the biosensing platform. Four different kinds of buffer were used in this work. The HBS-P buffer is the optimized buffer in this work, which contains 10 mM HEPES, 15 mM sodium chloride, 0.005 % Tween-20 and 0.1% BSA, pH was adjusted to 7.4. For comparison, HBS-EP,[1] PBS-P[2] and AH,[3] which are the commonly used buffers for the investigation of molecular interactions, were also tested. (a) Comparison of background signal generated in different buffers. Experiments were conducted in 20 μL working solution containing 10 μL of buffer, 5 μL donor beads (20 μg/mL) and 5 μL acceptor beads (20 μg/mL). Under this condition, the background signal generated in HBS-P buffer was about 9×10^3 RLU, which was 44.5%, 38.6%, and 29.1% lower than that of AH, HBS-EP, and PBS-P, respectively. (b) Comparison of ration of signal to noise (S/N) of the biosensor in different buffers. The 20 μL working solution contained 5 μL of each of the following ingredients: HucR (0.1 nM), Bio-*hucO* (1 nM), donor beads (20 μg/mL), and acceptor beads (20 μg/mL). Under this condition, HBS-P gave the highest S/N of 25.5, which was 2.08, 4.46 and 1.40-fold of those in AH, HBS-EP, and PBS-P, respectively. Since an appropriate working buffer should provide low background signal and high S/N, HBS-P buffer was finally chosen.

References

1 L. Wang, X. Tian, J. Wang, H. Yang, K. Fan, G. Xu, K. Yang, H. Tan, *Proc. Nat.l Acad. Sci. U. S. A.*, 2009, **106**, 8617-8622.

2 Y. Zhang, G. Pan, Z. Zou, K. Fan, K. Yang, H. Tan, *Mol. Microbiol.*, 2013, **90**, 884-897.

3 V. G. D'Agostino, V. Adami, A. Provenzani, *PLoS One*, 2013, **8**, e72426.

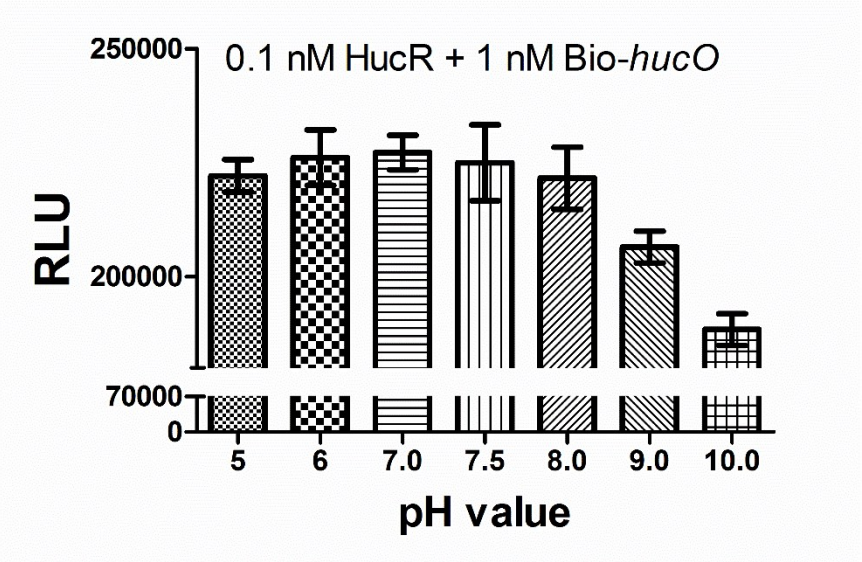

Fig. S5. Influence of pH on stability of the biosensing platform. Experiments were carried out in HBS-P buffer with different pH values. The 20 μL working solution contained 5 μL of each of the following ingredients: HucR (0.1 nM), Bio-*hucO* (1 nM), donor beads (20 μg/mL), and acceptor beads (20 μg/mL). No significant change of luminescence signals were observed when pH varied from 5.0 to 8.0, despite a slight signal decrease happened at pH 9.0 and 10.0. Significance was analyzed using Tukey's multiple comparison test.

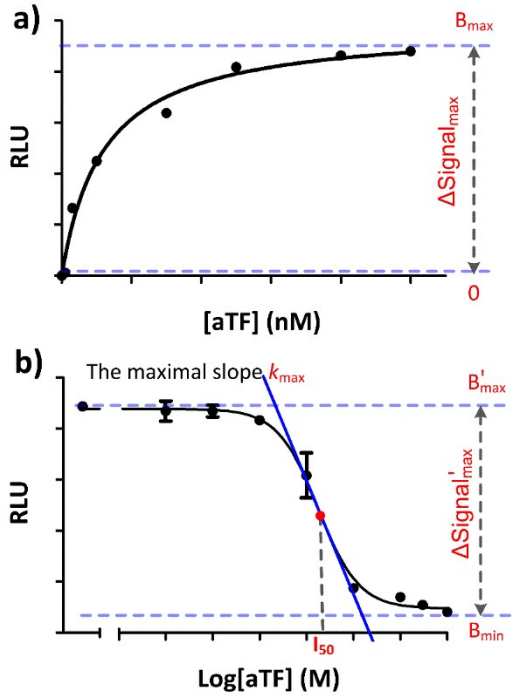

Fig. S6. Illustration of the curve of two equilibriums in the aTF-based biosensor. (a) Binding curve, which describes the binding of the aTF to its TFBS. (b) Dissociation curve, which depicts the dissociation of the aTF from its TFBS in the presence of effector (the target chemical).

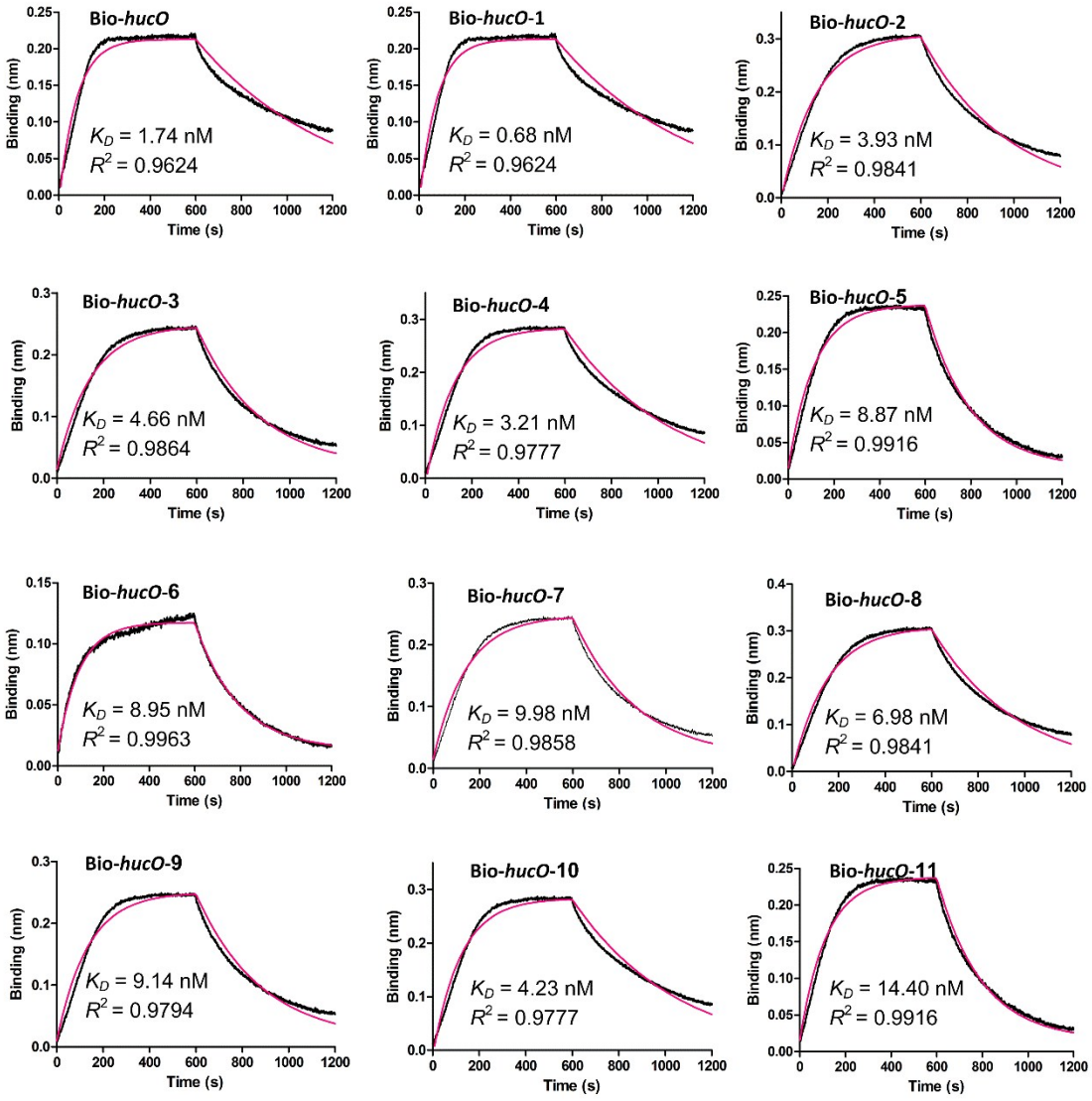

Fig. S7-1. Interaction behaviors between HucR and Bio-*hucO*, as well as its different mutants. Experiments were implemented by BLI technology. Bio-*hucO* and its mutants (10 ng/μL) were loaded on streptavidin sensor, and then interacted with HucR protein. The HucR concentrations were 10 nM. Blank experiments for data correction were carried out by using HBS-EP buffer instead of HucR in the binding step. Black and red lines indicate the experimental and fitted data, respectively.

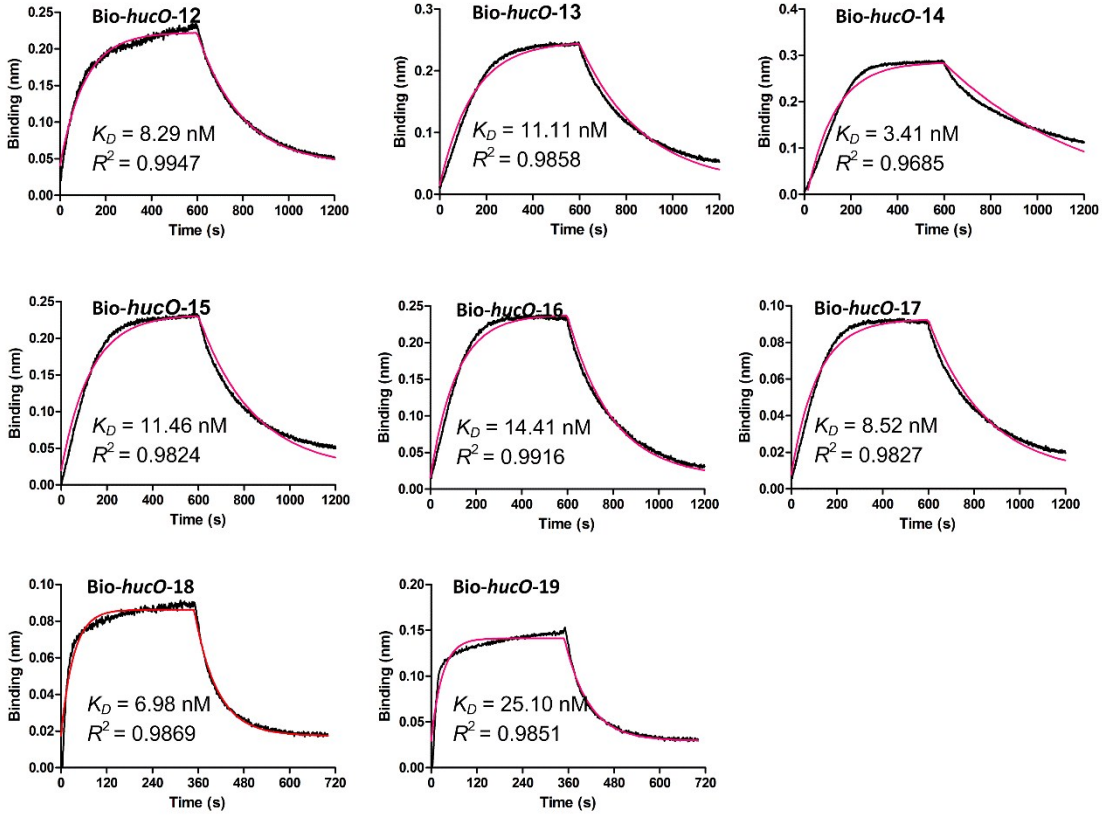

Fig. S7-2. Interaction behavior between HucR and Bio-*hucO*, as well as its different mutants. Experiments were implemented by BLI technology. Bio-*hucO* and its mutants (10 ng/μL) were loaded on streptavidin sensor, and then interacted with HucR protein. The HucR concentrations for interactions were 10 nM and 30 nM for Bio-*hucO* mutants Bio-*hucO*-12 to Bio-*hucO*-17, and Bio-*hucO*-18 to Bio-*hucO*-23, respectively. As no interaction between HucR and Bio-*hucO*-20 to Bio-*hucO*-23 was observed, data were not shown in this figure. Blank experiments for data correction were carried out by using HBS-EP buffer instead of HucR in the binding step. Black and red lines indicate the experimental and fitted data, respectively.

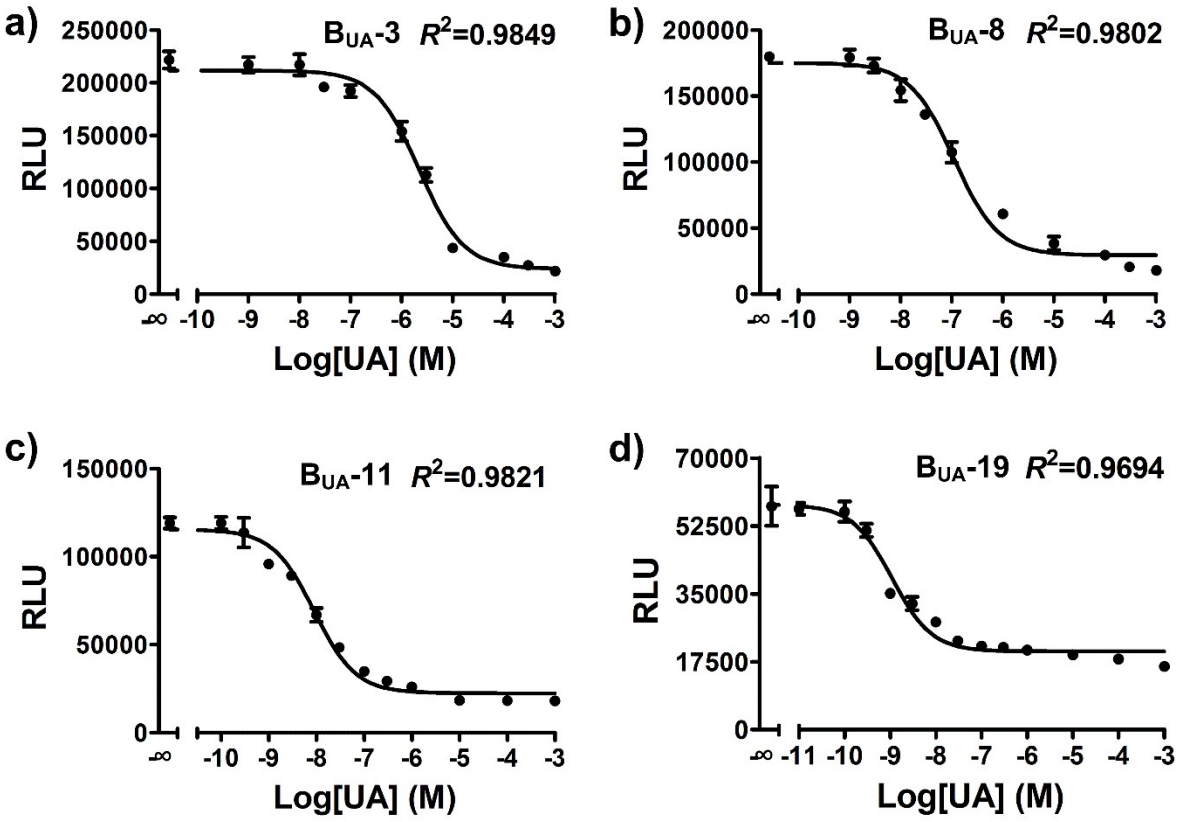

Fig. S8. Responses of four optimized UA biosensors to UA. (a) The optimized UA biosensor B_{UA}-3. (b) The optimized UA biosensor B_{UA}-8. (c) The optimized UA biosensor B_{UA}-11. (d) The optimized UA biosensor B_{UA}-19.

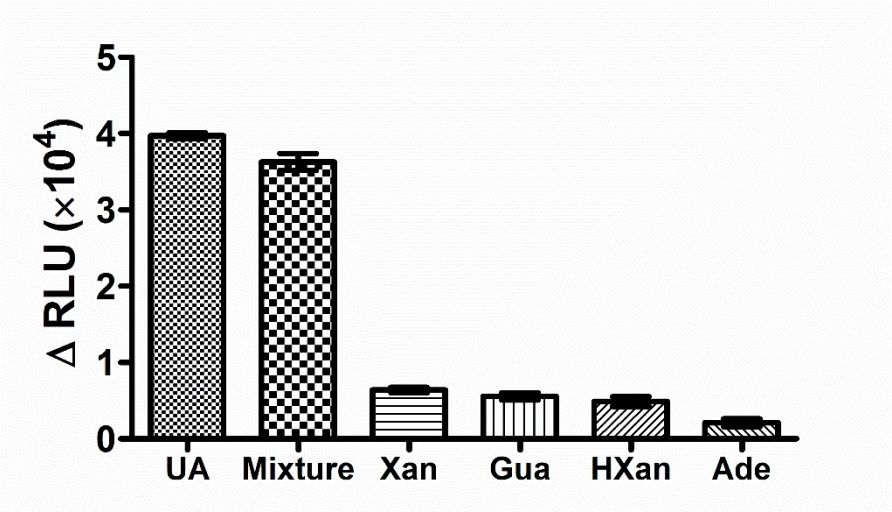

Fig. S9 Evaluation of the specificity of the HucR-based UA biosensor. B_{UA}-11 was used here because of its highest sensitivity and appropriate linear detection range. Experiments were carried out in the 25 μL working solution contained 5 μL of each of the following ingredients: HucR (0.1 nM), Bio-*hucO*-11 (1 nM), donor beads (20 μg/mL), and acceptor beads (20 μg/mL), and the tested chemicals. The concentrations of the tested chemicals are 10 nM for Xanthine (Xan), Guanine (Gua), hypoxanthine (HXan), and Adenine (Ade), and 1 nM for UA. ΔRLU was the change of luminescence signals of each experiment compared to the control, which used 5 μL HBS-P buffer instead of the tested chemicals in the same 25 μL working solution.

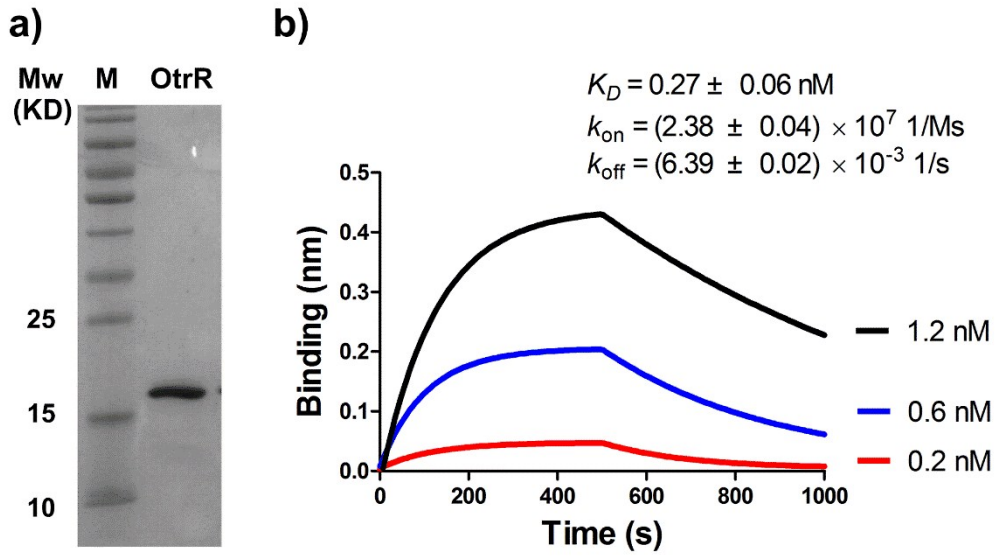

Fig. S10. Purified OtrR and its affinity to *otrO*. (a) Purified His_6-tagged OtrR examined by SDS-PAGE. Lane M, protein markers. (b) Determination of the affinity of OtrR for *otrO* by BLI. The Bio-*otrO* (10 ng/μL) was loaded on the streptavidin sensor, and then interacted with OtrR at three different concentrations of 1.2 nM (black line), 0.6 nM (blue line), and 0.2 nM (red line). The blank experiment for data correction was carried out by using HBS-EP buffer instead of OtrR in the binding step.

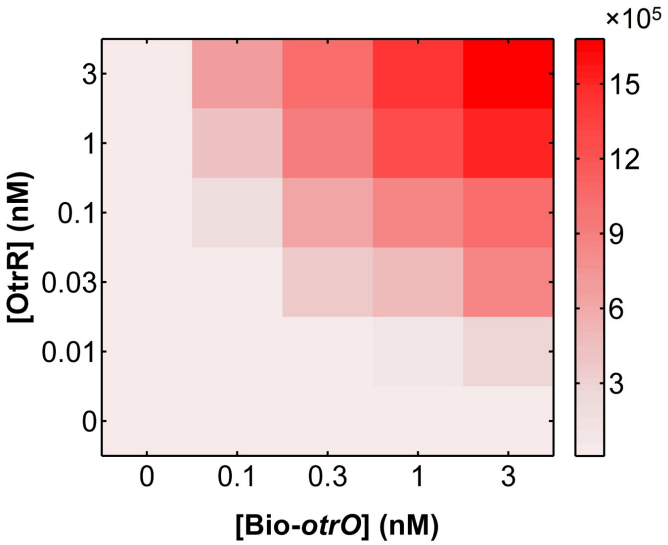

Fig. S11. Cross-titration of OtrR and Bio-*otrO* at different concentrations. The heat map describes the RLU generated under different concentrations. Experiments were carried out in the 20 μL working solution, containing 5 μL of each of the following ingredients: OtrR (0.1 nM), Bio-*otrO* (1 nM), donor beads (20 μg/mL), and acceptor beads (20 μg/mL). Under the condition of 0.03 nM OtrR and 0.3 nM Bio-*otrO*, luminescence and S/N was about 3.6×10^5 RLU and 42.1, respectively, which could fulfill the requirements of configuration of a biosensor. However, luminescence and S/N generated by 0.01 nM OtrR and 0.1 nM Bio-*otrO* was less than 2×10^4 and 3.0. Thus 0.03 nM OtrR and 0.3 nM Bio-*otrO* were finally chosen to configure OTC biosensors.

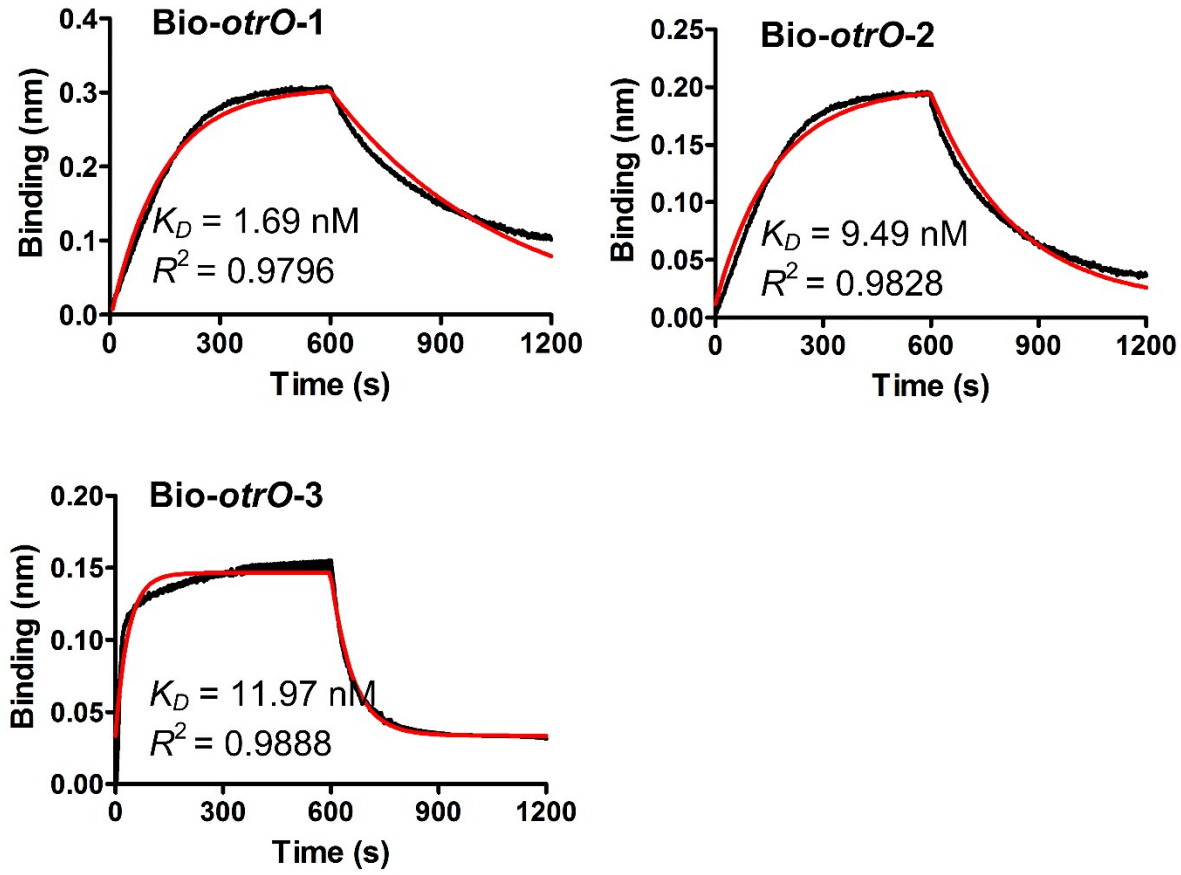

Fig. S12. Interaction behavior between OtrR and different mutants of Bio-*otrO***.** Experiments were implemented by BLI technology. Bio-*otrO* mutants (10 ng/μL) were loaded on streptavidin sensor, and then interacted with OtrR protein. The OtrR concentrations for interactions were 4 nM for Bio-*otrO*-1 and Bio-*otrO*-2, and 8 nM for Bio-*otrO*-3, respectively. Blank experiments for data correction were carried out by using HBS-EP buffer instead of OtrR in the binding step. Black and red lines indicate the experimental and fitted data, respectively.

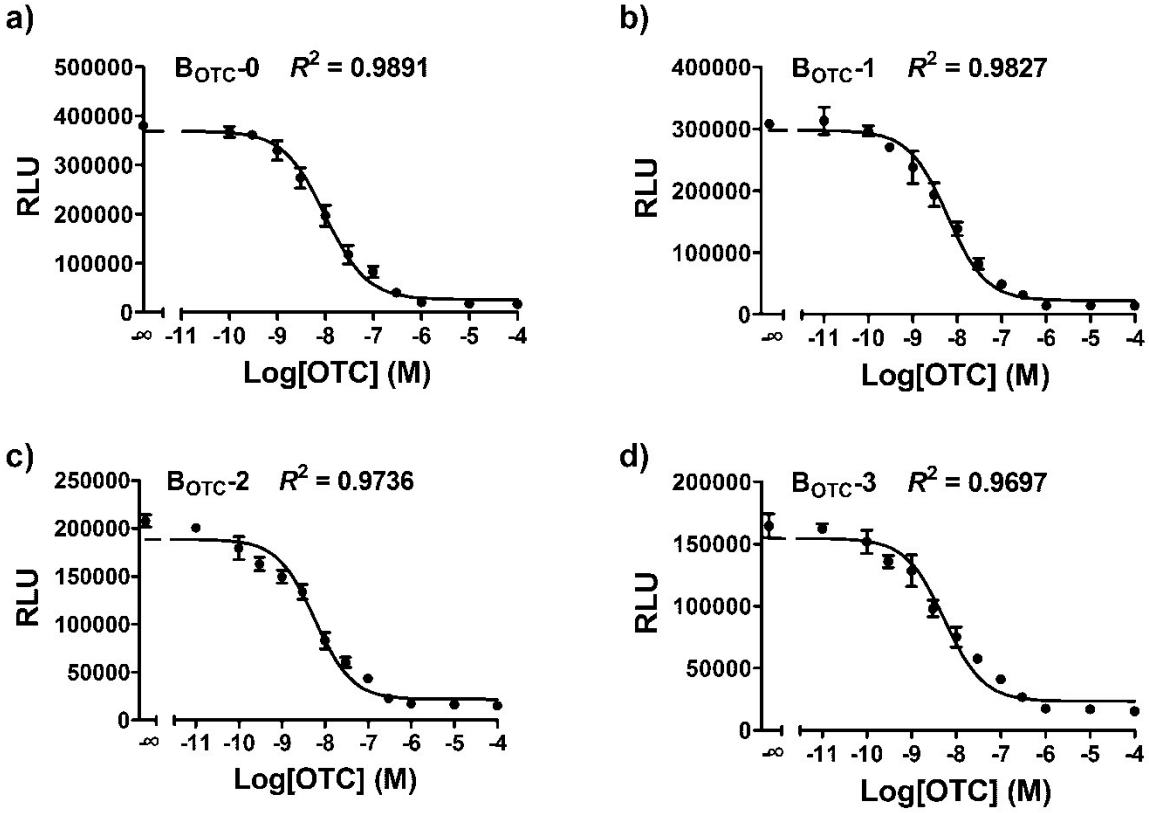

Fig. S13. Response of different OTC biosensors to OTC. (a) The original OTC biosensors B_{OTC}-0. (b) The optimized OTC biosensor B_{OTC}-1. (c) The optimized OTC biosensor B_{OTC}-2. (d) The optimized OTC biosensor B_{OTC}-3.

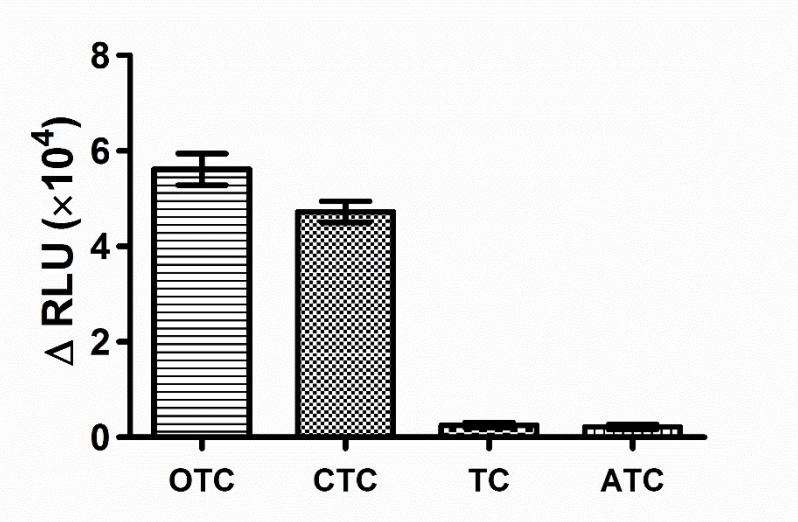

Fig. S14. Evaluation of the specificity of the OtrR-based OTC biosensor. B_{OTC}-2 was used here because of its highest sensitivity and appropriate linear detection range. Experiments were carried out in the 25 μL working solution contained 5 μL of each of the following ingredients: OtrR (0.03 nM), Bio-*otrO*-2 (0.3 nM), donor beads (20 μg/mL), and acceptor beads (20 μg/mL), and the tested chemicals. The concentrations for oxytetracycline (OTC), chlortetracycline (CTC), tetracycline (TC), and anhydrotetracycline (ATC) were all 1 nM. ΔRLU was the change of luminescence signals of each experiment compared to the control, which used 5 μL HBS-P buffer instead of the tested chemicals in the same 25 μL working solution.

Supporting tables

Table S1. Primers used in this work

Name	Sequence (5'-3')
BioP	CACACACGTTGTTCACCATC
RF	GATATACATATGAGCGCGCGCATGGATAACGATAC
RR	TGGTGCTCGAGAACACCCTGTTCGAGGCCCGCCAG
OF	CACACACGTTGTTCACCATCAGCAACAGTGCTACACTGCG
OR0	TGCCGCCGCCAGATACTTAGATGTCTACCTACTGAGGGCCGCAGTGTAGCACTGTTGCT
OR1	TGCCGCCGCCAGATACTTAGATGTCTAAGTACTGAGGGCCGCAGTGTAGCACTGTTGCT
OR2	TGCCGCCGCCAGATAGGTAGATGTCTACCTACTGAGGGCCGCAGTGTAGCACTGTTGCT
OR3	TGCCGCCGCCAGATACGTAGATGTCTACCTACTGAGGGCCGCAGTGTAGCACTGTTGCT
OR4	TGCCGCCGCCAGATACTTAGATGTCTACGTACTGAGGGCCGCAGTGTAGCACTGTTGCT
OR5	TGCCGCCGCCAGATACGAAGATGTCTACCTACTGAGGGCCGCAGTGTAGCACTGTTGCT
OR6	TGCCGCCGCCAGATACGTCGATGTCTACCTACTGAGGGCCGCAGTGTAGCACTGTTGCT
OR7	TGCCGCCGCCAGATACGTATATGTCTACCTACTGAGGGCCGCAGTGTAGCACTGTTGCT
OR8	TGCCGCCGCCAGATACTTAGCTGTCTACGTACTGAGGGCCGCAGTGTAGCACTGTTGCT

OR9	TGCCGCCGCCAGAGACTTAGATGTCTACGTACTGAGGGCCGCAGTGTAGCACTGTTGCT
OR10	TGCCGCCGCCAGATACTTAGATGTCTTCCTACTGAGGGCCGCAGTGTAGCACTGTTGCT
OR11	TGCCGCCGCCAGATACTTAGATGTCAACCTACTGAGGGCCGCAGTGTAGCACTGTTGCT
OR12	TGCCGCCGCCAGATACTTAGATGTGTACCTACTGAGGGCCGCAGTGTAGCACTGTTGCT
OR13	TGCCGCCGCCAGACACTTAGATGTCTACCTACTGAGGGCCGCAGTGTAGCACTGTTGCT
OR14	TGCCGCCGCCAGATGCTTAGATGTCTACCTACTGAGGGCCGCAGTGTAGCACTGTTGCT
OR15	TGCCGCCGCCAGATACTTAGCTGTCTACCTACTGAGGGCCGCAGTGTAGCACTGTTGCT
OR16	TGCCGCCGCCAGATACTGCGATGTCTACCTACTGAGGGCCGCAGTGTAGCACTGTTGCT
OR17	TGCCGCCGCCAGATACTGAGATGGCTACCTACTGAGGGCCGCAGTGTAGCACTGTTGCT
OR18	TGCCGCCGCCAGATACTGAGATGTATACCTACTGAGGGCCGCAGTGTAGCACTGTTGCT
OR19	TGCCGCCGCCAGATACTTAGATGACGACCTGCTGAGGGCCGCAGTGTAGCACTGTTGCT
OR20	TGCCGCCGCCAGACACTGCTATGTCTAAGCACTGAGGGCCGCAGTGTAGCACTGTTGCT
OR21	TGCCGCCGCCAGATACTTGGTTGTCTGCGTCCTGAGGGCCGCAGTGTAGCACTGTTGCT
OR22	TGCCGCCGCCAGATGCTTCGATGTATGAGTACTGAGGGCCGCAGTGTAGCACTGTTGCT
OR23	TGCCGCCGCCAGATACTTAGTTGTCGAACTGCTGAGGGCCGCAGTGTAGCACTGTTGCT
P-hucOF	GTCAGACCGTCCGAGTCTGGTC
P-hucOR	CTTGATCTTCATGAGCTGCAC
otrOR0	GAGAACGACAAGACCTTGTCAAAGCTGATGGTGAACAACGTGTGTG
otrOR1	GAGAAC GACATGACCTTGGCAAAGCTGATGGTGAACAACGTGTGTG

otrOR2	GAGAACGACGTCACCTTGTCAAAGCTGATGGTGAACAACGTGTGTG
otrOR3	GAGAACCACAAGACCTGGAC AAAGCTGATGGTGAACAACGTGTGTG

Table S2. Influence of foreign substances on luminescence signal

Foreign substances	Change of luminescence signal (%)	Foreign substances	Change of luminescence signal (%)
Zn^{2+}	1.06	Sucrose	0.66
K^{+}	0.94	Methionine	1.42
NH_4^{+}	1.22	Alanine	0.87
Na^{+}	0.57	Histidine	0.93
Ca^{2+}	2.05	Leucine	0.74
Mg^{2+}	1.38	Serine	1.15

Note: The concentration of each tested foreign substance was 100 mM. For each ion and substance, change of luminescence signal was expressed with the coefficient of variation of three independent determinations.

Table S3. Kinetic parameters of interactions between HucR and different mutants of Bio-*hucO*

Number	TFBS (5'-3')	K_D (nM)	k_{on} (1/Ms) $\times 10^6$	k_{off} (1/s) $\times 10^{-3}$
Bio-*hucO*	TAGGTAGACATCTAAGTA	1.74±0.03	1.04±0.02	1.82±0.01
Bio-*hucO*-1	TACTTAGACATCTAAGTA	0.68±0.02	0.82±0.01	0.56±0.01
Bio-*hucO*-2	TAGGTAGACATCTACCTA	3.93±0.06	0.77±0.01	3.03±0.02
Bio-*hucO*-3	TAGGTAGACATCTACGTA	4.66±0.08	0.67±0.01	3.11±0.02
Bio-*hucO*-4	TACGTAGACATCTAAGTA	3.21±0.03	0.68±0.01	2.21±0.01
Bio-*hucO*-5	TAGGTAGACATCTTCGTA	8.87±0.38	0.81±0.03	7.19±0.09
Bio-*hucO*-6	TAGGTAGACATCGACGTA	8.95±0.10	0.59±0.01	5.25±0.02
Bio-*hucO*-7	TAGGTAGACATATACGTA	9.98±0.24	0.37±0.07	3.68±0.02
Bio-*hucO*-8	TACGTAGACAGCTAAGTA	6.98±0.13	0.39±0.01	2.73±0.02
Bio-*hucO*-9	TACGTAGACATCTAAGTC	9.14±0.24	0.39±0.01	3.58±0.03
Bio-*hucO*-10	TAGGAAGACATCTAAGTA	4.23±0.07	0.56±0.01	2.37±0.02
Bio-*hucO*-11	TAGGTTGACATCTAAGTA	14.4±0.15	0.46±0.01	6.63±0.12
Bio-*hucO*-12	TAGGTACACATCTAAGTA	8.29±0.07	0.53±0.09	4.38±0.04
Bio-*hucO*-13	TAGGTAGACATCTAAGTG	11.11±0.13	0.47±0.02	5.18±0.02
Bio-*hucO*-14	TAGGTAGACATCTAAGCA	3.41±0.07	0.54±0.01	1.85±0.02
Bio-*hucO*-15	TAGGTAGACAGCTAAGTA	11.46±0.31	0.36±0.01	4.15±0.03
Bio-*hucO*-16	TAGGTAGACATCGCAGTA	14.41±0.29	3.56±0.06	5.12±0.02
Bio-*hucO*-17	TAGGTATACATCTCAGTA	8.52±0.18	4.66±0.07	3.97±0.03
Bio-*hucO*-18	TAGGTAGCCATCTCAGTA	6.98±0.49	1.26±0.08	8.77±0.20
Bio-*hucO*-19	TACTCATACATCGAAGCA	25.10±0.69	1.44±0.06	7.25±0.10
Bio-*hucO*-20	CAGTTCGACAACTAAGTA	ND	ND	ND
Bio-*hucO*-21	CAGGTCGTCATCTAAGTA	ND	ND	ND

Bio-*hucO*-22	TGCTTAGACATAGCAGTG	ND	ND	ND
Bio-*hucO*-23	GACGCAGACAACCAAGTA	ND	ND	ND

Notes: Underline indicates the non-symmetrical base pair, and blue letters indicate the original non-symmetrical base pairs. The green and light gray letters indicate point mutation, and the 2-bp interval within the TFBS, respectively. ND stands for not detected.

Table S4. Major parameters of the UA biosensors

Parameter	B_{UA}-0	B_{UA}-3	B_{UA}-8	B_{UA}-11	B_{UA}-19
K_D (nM)	1.74	4.66	6.97	14.4	25.1
I_{50} (mM)	1.946	1.785	0.9064	0.597	0.1462
k_{max} ($\times 10^5$)	-9.02	-5.46	-2.21	-0.86	-0.37
K_I (μM)	1.78	1.69	1.57	1.46	1.39
LOD (nM)	100	50	10	1	1
Linear range (nM) $\times 10^3$	1-10	0.5-10	0.03-10	0.001-30	0.003-1

Note: Affinity of HucR for Bio-*hucO* was measured by BLI and K_D was calculated using a 1:1 model ($R^2 > 0.96$). I_{50} and K_I were determined with the in-built one-site competitive binding model ($R^2 > 0.93$) in GraphPad Prism 5.0. The k_{max} was determined according to [Eq. (**5**)S].

Table S5. Comparison with previously reported UA biosensors

Recognition elements	Transducing elements	Linear range (μM)	LOD (μM)	K_m (mM)	Time and References
Uricase	PBNPs/SPE	30-300	10	NR	2013[1]
Uricase	PS membrane/Au	5-105	NR	NR	2007[2]
Uricase	UCNPs	20-850	6.7	NR	2016[3]
Uricase	CS/PABA-PtNP/(Au–PB)REd/Au	0.2-250	0.1	NR	2014[4]
Uricase	PTH/CNT/CFE	2-100	0.8	NR	2014[5]
Uricase	PdAg NFs/rGO/GCE	1-150	0.081	NR	2015[6]
Uricase	Graphite/$Ru(bpy)_3^{2+}$	10-1000	3.1	NR	2013[7]
Uricase	HRP-CdS quantum dots	125-1000	125	NR	2015[8]
Uricase	GSH-capped CdTe NPs	0.22-6	0.1	NR	2016[9]
Uricase	Naf/Fc/GCE	0.5-600	0.23	0.014	2015[10]
Uricase	/PBNPs/MWCNT/Pani/Au	5-800	5	0.055	2012[11]
Uricase	ZnO:N	50-1000	40	0.1	2013[12]
Uricase	CuO/Pt/glass	50-1000	140	0.12	2012[13]
Uricase	ZnO:N	0-1000	90	0.13	2014[14]
Uricase	Ni/NiO/ITO/glass	50-1000	30	0.15	2014[15]
Uricase	NiO/Pt/Ti/glass	50-1000	110	0.17	2011[16]
Uricase	NiO/Pt/Ti/glass	50-1000	40	0.18	2014[17]
Uricase	Chi-CNTsNF/AgNPs/Au	1-400	1	0.21	2014[18]
Uricase	egg shell memebrane/O_2 electrode	4.0-640	2	0.33	2007[19]

Uricase	c-MWCNT/GEL/PVF/GCE	0.2-710	0.023	0.37	2015[20]
Uricase	PPy-Fc/Pt	1-50	0.5	0.44	2006[21]
Uricase	PANI-Ppy/Au	2.5-85	1	1.57	2008[22]
Uricase	AuNPs/Amino acid/Au	20-2500	7	1.78	2013[23]
aTF HucR	Alpha technology	0.001-30	0.001	/	This work

Note: K_m is the Michaelis–Menten constant. NR indicates not reported.

References

1 S. Piermarini, D. Migliorelli, G. Volpe, R. Massoud, A. Pierantozzi, C. Cortese, G. Palleschi, *Sens. Actuators B Chem.*, 2013, **179**, 170-174.

2 X. Wang, T. Hagiwara, S. Uchiyama, *Anal. Chim. Acta*, 2007, **587**, 41-46.

3 Q. Long, A. Fang, Y. Wen, H. Li, Y. Zhang, S. Yao, *Biosens. Bioelectron.*, 2016, **86**, 10-114.

4 W. Wang, C. Qin, Q. Xie, X. Qin, L. Chao, Y. Huang, M. Dai, C. Chen, J. Huang, J. Hu, *Analyst*, 2014, **139**, 2904-2911.

5 M. E. Ghica, C. M. Brett, *Talanta*, 2014, **130**, 198-206.

6 L. X. Chen, J. N. Zheng, A. J. Wang, L. J. Wu, J. R. Chen, J. J. Feng, *Analyst*, 2015, **140**, 3183-3192.

7 J. Ballesta-Claver, R. Rodriguez-Gomez, L. F. Capitan-Vallvey, *Analy. Chim. Acta*, 2013, **770**, 153-160.

8 N. E. Azmi, N. I. Ramli, J. Abdullah, M. A. Abdul Hamid, H. Sidek, S. Abd Rahman, N. Ariffin, N. A. Yusof, *Biosens. Bioelectron.*, 2015, **67**, 129-133.

9 D. Jin, M.-H. Seo, B. T. Huy, Q.-T. Pham, M. L. Conte, D. Thangadurai, Y.-I. Lee, *Biosens. Bioelectron.*, 2016, **77**, 359-365.

10 T. Ghosh, P. Sarkar, A. P. Turner, *Bioelectrochemistry,* 2015, **102**, 1-9.

11 R. Rawal, S. Chawla, N. Chauhan, T. Dahiya, C. S. Pundir, *Int. J. Biol. Macromol.*, 2012, **50**, 112-118.

12 K. Jindal, M. Tomar, V. Gupta, *Analyst*, 2013, **138**, 4353-4362.

13 K. Jindal, M. Tomar, V. Gupta, *Biosens. Bioelectron.*, 2012, **38**, 11-18.

14 K. Jindal, M. Tomar, V. Gupta, *Biosens. Bioelectron.*, 2014, **55**, 57-65.

15 K. Arora, M. Tomar, V. Gupta, *Analyst*, 2014, **139**, 4606-4612.

16 K. Arora, M. Tomar, V. Gupta, *Biosens. Bioelectron.*, 2011, **30**, 333-336.

17 K. Arora, M. Tomar, V. Gupta, *Analyst*, 2014, **139**, 837-849.

18 A. Numnuam, P. Thavarungkul, P. Kanatharana, *Anal. Bioanal. Chem.*, 2014, **406**, 3763-3772.

19 Y. Zhang, G. Wen, Y. Zhou, S. Shuang, C. Dong, M. M. F. Choi, *Biosens. Bioelectron.*, 2007, **22**, 1791-1797.

20 P. E. Erden, C. Kacar, F. Ozturk, E. Kilic, *Talanta*, 2015, **134**, 488-495.

21 S. Cete, A. Yasar, F. Arslan, *Artif. Cells Blood Substit. Immobil. Biotechnol.*, 2006, **34**, 367-380.

22 F. Arslan, *Sensors*, 2008, **8**, 5492-5500.

23 Y. Liu, M. Yuan, L. Liu, R. Guo, *Sens. Actuators B Chem.*, 2013, **176**, 592-597.

Table S6. Kinetic parameters of interaction between OtrR and different mutants of Bio-*otrO*

Number	TFBS (5'-3')	K_D (nM)	k_{on} (1/Ms) $\times 10^6$	k_{off} (1/s) $\times 10^{-3}$
Bio-*otrO*	GACAGGGTCTTGTC	0.26 ± 0.06	23.8±0.04	6.39±0.02
Bio-*otrO*-1	GCCAAGGTCATGTC	1.69 ± 0.03	1.24±0.13	2.09±0.01
Bio-*otrO*-2	GACAAGGTGACGTC	9.49 ± 0.41	0.45±0.01	4.27±0.03
Bio-*otrO*-3	GTCCAGGTCTTGTG	11.97 ± 0.32	1.37±0.03	16.59±0.00

Notes: The red letter indicates mutation and the non-symmetrical base pair. The light gray letter indicates the 2-bp interval within the TFBS.

Table S7. Comparison with previously reported OTC biosensors

Recognition elements	Transducing elements	Linear range (nM)	LOD (nM)	K_m (nM)	Time and Reference
aptamer	graphene oxide hydrogel	54.3-2171.8	54.3	NR	2016[1]
aptamer	silver nanoclusters	0.5-100	0.1	NR	2016[2]
aptamer	p-type semiconductor BiOI doped with graphene	4.0-150	0.9	NR	2015[3]
aptamer	gold nanoparticles	1.0-1000	1	NR	2015[4]
aptamer	luminescence resonance energy transfer from upconversion nanoparticles to SYBR Green I	0.21-21.7	0.12	NR	2015[5]
aptamer	gold nanoparticles	NR	0.1	9.61	2014[6]
aptamer	horseradish peroxidase	26.7-108.2	26.7	4.7	2014[7]
aptamer	electrochemical aptasensor	21.7-1303.1	NR	NR	2013[8]
aptamer	microfabricated cantilever array	1.0-100	0.2	NR	2013[9]
aptamer	polystyrene latex microspheres with proximity optical fibers	2.1-217178.8	217.2	NR	2010[10]
aptamer	gold nanoparticles	25-1000	25	NR	2010[11]
aptamer	gold interdigitated array (IDA) electrode chip	1-100	NR	NR	2009[12]
antibody	Immunosensors electrode	NR	27	NR	2013[13]
polymer	glucose oxidase amplifier	NR	9.3	NR	2011[14]
aTF OtrR	Alpha technology	0.1-300	0.03	/	This work

Note: NR, not reported. For convenient comparison, data of linear range and LOD with different units in original

references have been recalculated and transcformed into data with the same unit (nM).

References

1 B. Tan, H. Zhao, L. Du, X. Gan, X. Quan, *Biosens. Bioelectron.*, 2016, **83**, 267-273.

2 M. Hosseini, F. Mehrabi, M. R. Ganjali, P. Norouzi, *Luminescence*, 2016, DOI:10.1002/bio.3112.

3 K. Yan, Y. Liu, Y. Yang, J. Zhang, *Analy. Chem.*, 2015, **87**, 12215-12220.

4 H. B. Seo, Y. S. Kwon, J. E. Lee, D. Cullen, H. M. Noh, M. B. Gu, *Analyst*, 2015, **140**, 6671-6675.

5 H. Zhang, C. Fang, S. Wu, N. Duan, Z. Wang, *Anal. Biochem.*, 2015, **489**, 44-49.

6 Y. S. Kwon, N. H. Ahmad Raston, M. B. Gu, *Chem. Commun.*, 2014, **50**, 40-42.

7 C. H. Kim, L. P. Lee, J. R. Min, M. W. Lim, S. H. Jeong, *Biosens. Bioelectron.*, 2014, **51**, 426-430.

8 D. Zheng, X. Zhu, X. Zhu, B. Bo, Y. Yin, G. Li, *Analyst*, 2013, **138**, 1886-1890.

9 H. Hou, X. Bai, C. Xing, N. Gu, B. Zhang, J. Tang, *Analy. Chem.*, 2013, **85**, 2010-2014.

10 K. Kim, M. B. Gu, D. H. Kang, J. W. Park, I. H. Song, H. S. Jung, K. Y. Suh, *Electrophoresis*, 2010, **31**, 3115-3120.

11 Y. S. Kim, J. H. Kim, I. A. Kim, S. J. Lee, J. Jurng, M. B. Gu, *Biosens. Bioelectron.*, 2010, **26**, 1644-1649.

12 Y. S. Kim, J. H. Niazi, M. B. Gu, *Analy. Chim. Acta*, 2009, **634**, 250-254.

13 F. Conzuelo, S. Campuzano, M. Gamella, D. G. Pinacho, A. J. Reviejo, M. P. Marco, J. M. Pingarron, *Biosens. Bioelectron.*, 2013, **50**, 100-105.

14 J. Li, F. Jiang, Y. Li, Z. Chen, *Biosens. Bioelectron.*, 2011, **26**, 2097-2101.

Table S8. Comparison of urinary UA concentrations determined by HPLC and UA biosensors

Analytical approach	Concentration of UA (mM)			
	Sample 1	Sample 2	Sample 3	Sample 4
HPLC	3.34 ± 0.09	1.94 ± 0.06	1.53 ± 0.07	1.62 ± 0.04
B_{UA}-0	3.54 ± 0.10	1.86 ± 0.07	1.47 ± 0.04	1.56 ± 0.05
B_{UA}-3	3.42 ± 0.08	1.92 ± 0.06	1.49 ± 0.03	1.55 ± 0.08
B_{UA}-8	3.19 ± 0.12	2.06 ± 0.09	1.52 ± 0.06	1.69 ± 0.06
B_{UA}-11	3.24 ± 0.11	1.99 ± 0.08	1.59 ± 0.05	1.53 ± 0.04
B_{UA}-19	3.49 ± 0.10	2.02 ± 0.11	1.46 ± 0.07	1.51 ± 0.10

Note: The urine samples were collected from four healthy volunteers. Concentration was the average and standard derivation of three independent tests. The normal range of UA concentration ranges from 1.49 to 4.46 mM.[1]

Reference

1 N. E. Azmi, N. I. Ramli, J. Abdullah, M. A. Abdul Hamid, H. Sidek, S. Abd Rahman, N. Ariffin, N. A. Yusof, *Biosens. Bioelectron.*, 2015, **67**, 129-133.

Table S9. Evaluation of the performance of UA biosensors in urine samples

Approach	Accuracy (%)				Precision	Recovery
	Sample 1	Sample 2	Sample 3	Sample 4	(RSD%)	(%)
HPLC	100	100	100	100	/	/
B_{UA}-0	105.99	95.88	96.08	96.30	4.29	96.5
B_{UA}-3	102.40	98.97	97.39	95.68	2.48	98.2
B_{UA}-8	95.51	106.19	99.35	104.32	4.19	97.6
B_{UA}-11	97.01	102.58	103.92	94.44	3.90	101.1
B_{UA}-19	104.49	104.12	95.42	93.21	5.00	104.3

Note: Accuracy was determined by comparing the concentration determined by UA biosensors with that obtained by HPLC, which was fixed to 100%. For each biosensor, precision was the relative standard derivation (RSD) of accuracies generated from four different samples. Recovery tests were implemented by using 1 μM of UA.

Table S10. Evaluation of the performance of UA biosensors in human serum

Approach	Concentration (μM)		Accuracy (%)		Precision	Recovery
	Sample 1	Sample 2	Sample 1	Sample 2	(RSD%)	(%)
HPLC	94.05 ± 2.89	122.35 ± 6.55	100	100	/	/
B_{UA}-0	100.14 ± 8.42	133.24 ± 9.04	106.47	108.90	1.13	102.8
B_{UA}-3	84.26 ± 3.73	119.29 ± 8.61	89.59	97.50	4.23	95.2
B_{UA}-8	91.70 ± 6.75	111.93 ± 5.52	97.50	91.48	3.18	96.4
B_{UA}-11	88.53 ± 7.02	128.26 ± 9.23	94.13	104.83	5.38	101.5
B_{UA}-19	85.90 ± 5.41	119.77 ± 6.57	91.33	97.89	3.47	104.7

Note: Human serum with different brands (Solarbio, sample 1; LabLead, sample 2) were purchased from different suppliers (Beijing Solarbio Science & Technology Co., Ltd. and Beijing LabLead Biotech Co., Ltd.). Concentration was the average value and standard derivation of three independent tests. Accuracy was determined by comparing the concentration determined by UA biosensors with that obtained by HPLC, which was fixed to 100%. For each biosensor, precision was the relative standard derivation (RSD) of accuracies generated from two different samples. Recovery tests were implemented by using 1 μM of UA.

Table S11. List some of aTFs with various effectors in bacteria

aTFs	Effector	Binding sequences of aTFs	Strains and references
HucR	uric acid	TACTTAGATGTCTACCTA	*Deinococcus radiodurans*[1]
BetI	choline	TTAATTGAACGTTCAATTAA	*E. coli* BL21-AI[2]
AguR	agmatine	GTCCGATTTTTATCGGAT	*Pseudomonas aeruginosa* PAO1[3]
BepR	deoxycholate	AAAGTAAACTCGTTGGTGTACT	*Vibrio cholerae*[4]
HrtR	heme	ATGACACAGTGTCATAA	*Lactococcus lactis*[5]
BrtA	cholic acid	NR	Listeria monocytogenes[6]
RutR	uracil	TGGACTAAACGGTCAA	*E. coli*[7]
MerR	mercury	TATCGCTTGACTCCGTACATGAGTACGGAAGT AAGGT	*Pseudomonas transposon* Tn501[8]
ArsR	arsenite	ACACATTCGTTAAGTCATATATGTTTTTGACTT	*E. coli* K12[9]
CadC	zinc/cadmium	CACTCAAATAAATATTTGAATG	*Staphylococcus aureus*[10]
CadC1945	lead	TATATTCAAACATACACTTGAATAAA	*Bacillus oceanisediminis* 2691[11]
OtrR	oxytetracycline	TTGACAAGGTCTTGTCGTT	*Streptomyces rimosus*[12]
PmeR	flavonoid	TTACAAACAACCGCAATGTAA	*Pseudomonas syringae*[13]
TetR	tetracycline	ACTCTATCATTGATAGAGT	*E. coli* transposon Tn10[14]
MphR	erythromycin	GAATATAACCGACGTGACTGTTACATTTAG	*E. coli* Tf481A[15]

Pip	pristinamycin	TGTACAGCGTATAGGAAAGC	*Streptomyces coelicolor*[16]
NalC	chlorinated phenols	TAAGAACTGTATCGTACAGTACT	*P. aeruginosa* PAO1[17]
HosA	4-hydroxybenzoic Acid	CGTTCGTATACGAACA	*E. coli* UMN026[18]
HcaR	hydroxycinnamates; 3,4-dihydrobenzoate	CAATATCAGTTAAACTTACATTG	*Acinetobacter sp. ADP1*[19]
RolR	resorcinol	TGAACCCTTGTTCATTTATGAATCATGATTCA	*Corynebacterium glutamicum*[20]
SmeT	triclosan	GTTTACAAACAAACAAGCATGTATGTATAT	*Stenotrophomonas maltophilia*[21]

Note: NR indicates not reported.

References

1 S. P. Wilkinson, A. Grove, *J. Biol. Chem.*, 2004, **279**, 51442-51450.

2 K. Ike, Y. Arasawa, S. Koizumi, S. Mihashi, S. Kawai-Noma, K. Saito, D. Umeno, *ACS Synth. Biol.*, 2015, **4**, 1352-1360.

3 Y. Nakada, Y. Jiang, T. Nishijyo, Y. Itoh, C. D. Lu, *J. Bacteriol.*, 2001, **183**, 6517-6524.

4 F. A. Cerda-Maira, G. Kovacikova, B. A. Jude, K. Skorupski, R. K. Taylor, *J. Bacteriol.*, 2013, **195**, 307-317.

5 D. Lechardeur, B. Cesselin, U. Liebl, M. H. Vos, A. Fernandez, C. Brun, A. Gruss, P. Gaudu, *J. Biol. Chem.*, 2012, **287**, 4752-4758.

6 S. J. Quillin, K. T. Schwartz, J. H. Leber, *Mol. Microbiol.*, 2011, **81**, 129-142.

7 T. Shimada, A. Ishihama, S. J. Busby, D. C. Grainger, *Nucleic Acids Res.*, 2008, **36**, 3950-3955.

8 H. B. Guo, A. Johs, J. M. Parks, L. Olliff, S. M. Miller, A. O. Summers, L. Liang, J. C. Smith, *J. Mol. Biol.*, 2010, **398**, 555-568.

9 C. Xu, W. Shi, B. P. Rosen, *J. Biol. Chem.*, 1996, **271**, 2427-2432.

10 K. P. Yoon, T. K. Misra, S. Silver, *J. Bacteriol.*, 1991, **173**, 7643-7649.

11 H. J. Kim, J. W. Lim, H. Jeong, S. J. Lee, D. W. Lee, T. Kim, S. J. Lee, *Biosens. Bioelectron.*, 2016, **79**, 701-708.

12 W. Wang, T. Yang, Y. Li, S. Li, S. Yin, K. Styles, C. Corre, K. Yang, *ACS Synth. Biol.*, 2016, **5**, 765-773.

13 P. Vargas, A. Felipe, C. Michan, M. T. Gallegos, *Mol. Plant Microbe Interact.*, 2011, **24**, 1207-1219.

14 C. Kisker, W. Hinrichs, K. Tovar, W. Hillen, W. Saenger, *J. Mol. Biol.*, 1995, **247**, 260-280.

15 N. Noguchi, K. Takada, J. Katayama, A. Emura, M. Sasatsu, *J. Bacteriol.*, 2000, **182**, 5052-5058.

16 M. Folcher, R. P. Morris, G. Dale, K. Salah-Bey-Hocini, P. H. Viollier, C. J. Thompson, *J. Biol. Chem.*, 2001, **276**, 1479-1485.

17 S. Ghosh, C. M. Cremers, U. Jakob, N. G. Love, *Mol. Microbiol.*, 2011, **79**, 1547-1556.

18 A. Roy, A. Ranjan, *Biochemistry*, 2016, **55**, 1120-1134.

19 Y. Kim, G. Joachimiak, L. Bigelow, G. Babnigg, A. Joachimiak, *J. Biol. Chem.*, 2016, **291**, 13243-13256.

20 T. Li, K. Zhao, Y. Huang, D. Li, C. Y. Jiang, N. Zhou, Z. Fan, S. J. Liu, *Appl. Environ. Microb.*, 2012, **78**, 6009-6016.

21 A. Hernández, F. M. Ruiz, A. Romero, J. L. Martínez, *PLoS Pathog.*, 2011, **7**, e1002103.